

Analysis and Optimization of Random Cache in Multi-Antenna HetNets with Interference Nulling

Kangda Zhi^{*}, Guangji Chen^{*}, Ling Qiu^{*}, Xiaowen Liang^{*}, and Chenhao Ren[†]

^{*}School of Information Science and Technology, University of Science and Technology of China, Hefei, China.

[†] Department of Electrical and Computer Engineering, University of California, Davis, USA

Email: (kdzhi, chen0404)@mail.ustc.edu.cn, (lqiu, lxw)@ustc.edu.cn, cheren@ucdavis.edu

Abstract—From the perspective of statistical performance, this paper presents a framework for the per-user throughput analysis in random cache based multi-antenna heterogeneous networks (HetNets) with user-centric inter-cell interference nulling (IN). Using tools from stochastic geometry, an explicit expression for the per-user throughput is derived. Based on the analytical results, the optimal cache probabilities for maximizing the per-user throughput are analyzed. Theoretical analysis and numerical results reveal that the optimal random cache under interference nulling fully harvests the file diversity gain (FDG) and achieves a promising per-user throughput.

Index Terms—Cache, inter-cell interference nulling, multi-antenna, heterogeneous wireless networks, stochastic geometry.

I. INTRODUCTION

Heterogeneous networks (HetNets) and multi-antenna have been recognized as two key technologies to meet the predicted throughput requirements in 5G networks [1]. However, rapidly growing traffic makes the backhaul rate a major bottleneck in implementing these technologies in practical systems. To address these problems, caching has been recognized as a promising technology to reduce the backhaul traffic and achieve low latency by avoiding duplicate delivery of popular content [2].

Recently, contrasted to traditional grid model, a random network model based on Poisson point processes (PPPs) has been widely applied in cache-enabled small cell networks to characterize the irregularity and randomness of base station (BS) locations [3]–[6]. These works proposed and analyzed some traditional cache placement schemes, such as the most popular cache (MPC) scheme [3] [4], the uniform cache (UC) scheme [5] and the i.i.d. cache (IIDC) scheme [6]. However, these cache schemes [3]–[6] cannot sufficiently exploit the finite storage capacity, and may not yield optimal network performance. In contrast, random cache (RC) scheme has been proved to achieve better performance by leveraging file diversity and file popularity. Recent contributions have considered the analysis and optimization of various performance metrics in random cache based small cell networks, e.g. the throughput [7], the hit probability [8], and the successful transmission probability (STP) [9]. Note that [7]–[9] focus on the scenarios without interference management.

Interference management is critical in random cache based networks. This is because when the nearest BS does not cache the requested content, the user will be served by a relatively farther BS, which makes the signal usually weaker than the interference. To increase received signal power under random cache, [10] [11] jointly considered random cache and cooperative transmission to optimize the STP in HetNets. Nevertheless, [10] [11] are studied without considering the multi-antenna. To take advantages of multiple antennas, [12] adopted maximal ratio transmission (MRT) beamforming to boost the desired signal in multi-antenna cache-enabled networks with limited backhaul. Moreover, part of the degree of freedom (DoF) can be utilized to avoid those dominant interference in cache-enabled networks. Adopting coordinated beamforming (CBF), [13] considered the analysis and optimization of STP in multi-antenna cache-enabled networks, where a certain number of small base stations (SBSs) form the coordination cluster. However, none of the aforementioned literatures has addressed the analysis and optimization of per-user throughput, which is an important performance metric in cache-enabled networks [2].

In addition, the CBF scheme adopted by [13] ignored the “BS selection conflict problem” in dynamic clustering, i.e., a joint BS shared by different clusters can be selected by different users who share the same spectrum at the same time. Although this problem can be solved by allocating orthogonal time-frequency resources to adjoint clusters [14], it will result in a reduction in the per-user available bandwidth. Therefore, the scheme in [13] may not be suitable for throughput maximization. Recently, [15], [16] proposed a tractable interference nulling (IN) strategy in traditional networks with connection-based association scheme. [15], [16] used random elimination strategy to treat the BS selection conflict problem, which can avoid the reduction of throughput. However, these IN strategies cannot be directly applied to cache-enabled HetNets with content-centric association scheme, as different association schemes result in different distributions of the locations of serving and interfering BSs, and hence lead to different geographic locations of the dominant interference. Therefore, to fully utilize the storage capacity and achieve promising per-user throughput, further research is required to apply IN to random cache based HetNets and understand the relationship between random cache and IN.

In this paper, we apply the user-centric inter-cell IN strat-

This work was supported by National Natural Science Foundation of China under Grant No.61672484. (Corresponding author: Ling Qiu.)

egy to random cache based HetNets and jointly investigate the benefits of random cache and IN. Employing IN, each SBS utilizes zero-forcing beamforming (ZFBF) to avoid the interference to nearby SBS scheduled users. Since the cache-enabled networks aim at efficient content delivery [8], we analyze and optimize the per-user throughput. Our main contributions are summarized as follows:

- We present a framework for the per-user throughput analysis in random cache based multi-antenna HetNets with user-centric inter-cell IN.
- By carefully handling the different types of interfering SBSs and employing appropriate approximations, we theoretically derive the explicit expressions for the per-user throughput based on stochastic geometry, which can be easily calculated through mathematical software.
- The optimal cache placement is obtained via standard optimization techniques. The optimization results indicate that more different contents can be cached in the SBS tier when SBSs are equipped with more antennas.
- By numerical results, we analyze the influences of various system parameters, including physical-layer related parameters and content-layer related parameters. Moreover, we show that the benefits brought by random cache are enhanced by the IN. The results show that joint random cache and IN can achieve a significant gain in the per-user throughput over existing baseline schemes.

II. SYSTEM MODEL

We consider a downlink two-tier HetNets where macro base stations (MBSs) are overlaid with small base stations (SBSs). The locations of MBSs and SBSs are modeled as two independent PPPs Φ_0 and Φ_1 with densities λ_0 and λ_1 , respectively. The MBSs and SBSs are equipped with N_0 and N_1 antennas, respectively. The single antenna users are located according to an independent PPP Φ_u with λ_u , where $\lambda_u \gg \lambda_1 > \lambda_0$. We assume that all BSs are fully loaded and active as in [9], [10], [12]. Without loss of generality, we focus on the typical user u_0 located at the origin.

Let $\mathcal{F} \triangleq \{1, 2, \dots, F\}$ denote the set of F files in the network. For ease of illustration, all files are assumed to have the equal unit size as [7], [8], [11]–[13]. We assume that the popularity a_n of the file n is arranged in a descending order according to the law of Zipf as [7]–[13], i.e., $a_n = \frac{n^{-\gamma}}{\sum_{i \in \mathcal{F}} i^{-\gamma}}$, where the Zipf exponent γ represents the skewness of the popularity distribution. We assume that each MBS is equipped with no cache but is connected to the core network through backhaul link with high capacity. Each SBS is equipped with a cache of size C , where $C \leq F$. A random cache strategy is adopted where each SBS independently caches file $n \in \mathcal{F}$ with probability $T_n \in [0, 1]$, and we have $\sum_{n \in \mathcal{F}} T_n \leq C$ due to the cache storage limit. Hereafter, $\mathbf{T} \triangleq (T_n)_{n \in \mathcal{F}}$ is referred to as “cache distribution”. Denote $\mathcal{F}^+ \triangleq \{n | n \in \mathcal{F}, T_n > 0\}$, hence $|\mathcal{F}^+|$ represents the number of different files could be stored in the SBS tier.

The user who requests file n is associated with the nearest SBS cached file n within R_c , where R_c is the distance threshold used to define the maximum service distance for the SBSs. Specifically, if no SBS within R_c stores the requested file, the nearest MBS will retrieve file from the core network and then fulfill the user request. After the user association, each BS schedules its associated users according to TDMA, i.e., scheduling one user in each time slot. Therefore, there is no intra-cell interference.

Orthogonal frequencies are applied at MBSs and SBSs to avoid inter-tier interference. The available bandwidths of each MBS and SBS for u_0 are W_m and W_s , respectively. Similar to [10], we assume $W_s > W_m$. To suppress those dominant interference within the SBS tier, we consider a user-centric inter-cell interference nulling strategy, assuming each SBS uses ZFBF to avoid interference with neighboring users. Considering that in the cache-enabled networks, dominant interferences come from the SBSs that are closer than the serving SBS, thus the user associated with SBS tier will send an interference mitigation request to all the interfering SBSs within distance R_c . Each SBS can handle at most $N_1 - 1$ requests due to spatial DoF constraint. Let K_x represent the number of requests received by SBS x , if $K_x \geq N_1$, we assume that SBS x will randomly choose $N_1 - 1$ users to suppress interference. Therefore, SBS x will use $\max(N_1 - K_x, 1)$ DoF to boost the desired signal to its scheduled user. Note that if $K_x = 0$, SBS x will utilize maximal ratio transmission (MRT) precoding to serve its scheduled user.

In this paper, we consider the interference-limited regime and hence ignore the thermal noise. For notation simplicity, we use number 0 and 1 to distinguish the MBS tier and the SBS tier. We denote the serving BS of u_0 associated with tier z as BS $x_{z,0}$, where $z \in \{0, 1\}$. When the typical user u_0 is associated with the SBS $x_{1,0}$, different from the conventional connection-based networks, there are three types of interferers. Let Φ_1^1 denote the set of interfering SBSs closer than serving SBS $x_{1,0}$, Φ_1^2 denote the set of interfering SBSs farther than $x_{1,0}$ but closer than R_c , and Φ_1^3 denote the set of interfering SBSs farther than R_c . Note that Φ_1^1 and Φ_1^2 are the set of SBSs who receive the IN request from u_0 but cannot mitigate interference for u_0 due to the limitation of DoF. Then the received signal of u_0 associated with tier 1 is given by:

$$y_{1,0} = |x_{1,0}|^{-\frac{\alpha_1}{2}} \mathbf{h}_{x_{1,0}}^* \mathbf{w}_{x_{1,0}} s_{x_{1,0}} + \sum_{x_{1,j} \in \Phi_1^1 \cup \Phi_1^2 \cup \Phi_1^3} |x_{1,j}|^{-\frac{\alpha_1}{2}} \mathbf{h}_{x_{1,j}}^* \mathbf{w}_{x_{1,j}} s_{x_{1,j}}, \quad (1)$$

where $\mathbf{h}_x \in \mathcal{CN}(\mathbf{0}_{N_1 \times 1}, \mathbf{I}_{N_1})$ denotes the small-scale fading between SBS x and u_0 , $|x|$ denotes the distance from BS x to u_0 , $|x|^{-\frac{\alpha_1}{2}}$ represents the large-scale path loss, where $\alpha_1 > 2$ is the path loss exponent, s_x is the information symbol from SBS x to u_0 , and \mathbf{w}_x denotes the beamforming vector for SBS x .

We assume that serving SBS $x_{1,0}$ receives $K_{x_{1,0}}$ IN requests, and SBS $x_{1,0}$ will handle $\min(K_{x_{1,0}}, N_1 - 1)$ IN

requests. Then the ZF beamforming vector $\mathbf{w}_{x_{1,0}}$ is given by:

$$\mathbf{w}_{x_{1,0}} = \frac{\left(\mathbf{I}_{N_1} - \mathbf{H}(\mathbf{H}^* \mathbf{H})^{-1} \mathbf{H}^* \right) \mathbf{h}_{x_{1,0}}}{\left\| \left(\mathbf{I}_{N_1} - \mathbf{H}(\mathbf{H}^* \mathbf{H})^{-1} \mathbf{H}^* \right) \mathbf{h}_{x_{1,0}} \right\|}, \quad (2)$$

where $\mathbf{H} = [\mathbf{h}_1, \dots, \mathbf{h}_{\min(K_{x_{1,0}}, N_1 - 1)}]$ is the channels between SBS $x_{1,0}$ and $\min(K_{x_{1,0}}, N_1 - 1)$ selected users, and \mathbf{H}^* is the conjugate transpose of \mathbf{H} .

However, if no SBS within R_c stores the requested file, u_0 will be associated with tier 0 and served by the nearest MBS $x_{0,0}$ that utilizes MRT precoding. In this case, the form of received signal is similar to that in [12]. Therefore, the signal-to-interference ratio (SIR) of u_0 associated with tier z is $\text{SIR}_z = \frac{S_z}{I_z}$, $z \in \{0, 1\}$, i.e.,

$$\text{SIR}_0 = \frac{g_{x_{0,0}} |x_{0,0}|^{-\alpha_0}}{\sum_{x_{0,j} \in \Phi_0 \setminus x_{0,0}} g_{x_{0,j}} |x_{0,j}|^{-\alpha_0}}, \quad (3)$$

$$\text{SIR}_1 = \frac{g_{x_{1,0}} |x_{1,0}|^{-\alpha_1}}{\sum_{x_{1,j} \in \Phi_1 \cup \Phi_2 \cup \Phi_3} g_{x_{1,j}} |x_{1,j}|^{-\alpha_1}}. \quad (4)$$

Here, $g_{x_{z,j}}$, $z \in \{0, 1\}$ is the equivalent channel gain from BS $x_{z,j}$ to user u_0 , including channel coefficients and the beamforming. α_z is the path loss exponent. According to [15] [16], the information signal channel gain $g_{x_{z,0}}$ follows Gamma distributed, i.e., $g_{x_{0,0}} \sim \text{Gamma}(N_0, 1)$ and $g_{x_{1,0}} \sim \text{Gamma}(\max(N_1 - K_{x_{1,0}}, 1), 1)$, and the interfering channel gain $g_{x_{z,j}}$, $z \in \{0, 1\}$ is exponential distributed with mean 1.

III. ANALYSIS OF PER-USER THROUGHPUT

In this section, we will derive the expression of the per-user throughput under a given cache distribution. The per-user throughput of the typical user is given by

$$R(\mathbf{T}) = \sum_{n \in \mathcal{F}} a_n (W_m P_m^n R_0^n + W_s P_s^n R_1^n), \quad (5)$$

where R_0^n and R_1^n denote the average spectral efficiency when typical user requesting file n is served by MBS and SBS, respectively, P_m^n refers to the probability that typical user requesting file n is served by MBS, and P_s^n denotes the ‘‘cache hit probability’’, i.e., there is an SBS caching the requested file n and within cooperation region (i.e., within R_c).

Before calculating throughput, we will first characterize the distribution of the crucial parameter K_x . To make the analysis tractable, we make the following approximations:

Approximation 1: The scheduled micro users form a homogeneous PPP Φ_u^1 with density λ_1 .

Approximation 2: The numbers of IN requests received by different SBSs are independent.

Similar approximations have been adopted in traditional connection-based networks as [15]–[17], and their accuracy in content-centric networks will be verified in Section V. With Approximation 1, since SBS x will receive the IN requests from scheduled users at distance r away from SBS x if $r < R_c$, K_x is a Poisson distributed variable with parameter

$\bar{K} = \pi R_c^2 \lambda_1$. Then, we can obtain the probability mass function of K_x , i.e., $p_K(k) = \frac{(\pi R_c^2 \lambda_1)^k}{k!} e^{-\pi R_c^2 \lambda_1}$.

Based on $p_K(k)$, the probability that a SBS received the request from u_0 but can not eliminate the interference for u_0 , i.e., the interference residual ratio, can be calculated as follows:

$$\varepsilon = \sum_{k=N_1-1}^{\infty} \frac{k+1-(N_1-1)}{k+1} p_K(k). \quad (6)$$

Based on the thinning theory of PPP and Approximation 2, when u_0 requests file n , the densities of three types of interfering SBSs Φ_1^1 , Φ_1^2 and Φ_1^3 , i.e., $\lambda_1^1(x)$, $\lambda_1^2(x)$ and $\lambda_1^3(x)$ can be obtained as follows:

$$\begin{aligned} \lambda_1^1(x) &= \lambda_1 (1 - T_n) \varepsilon \mathbb{1}(\|x\| \in [0, x_{1,0})), \\ \lambda_1^2(x) &= \lambda_1 \varepsilon \mathbb{1}(\|x\| \in [x_{1,0}, R_c)), \\ \lambda_1^3(x) &= \lambda_1 \mathbb{1}(\|x\| \in [R_c, \infty)), \end{aligned} \quad (7)$$

where $\mathbb{1}(\ast)$ denotes the indicator function. Aided by the above results, we derive the per-user throughput based on the tools from stochastic geometry.

Theorem 1: In the cache-enabled multi-antenna HetNets with user-centric inter-cell interference nulling strategy, the per-user throughput is given by

$$R(\mathbf{T}) = \sum_{n \in \mathcal{F}} a_n (f_m(T_n) + f_s(T_n)), \quad (8)$$

with

$$f_m(T_n) = W_m e^{-\pi T_n \lambda_1 R_c^2} \int_0^{\infty} \frac{(1 - (1+t)^{-N_0})}{t \left(1 + \frac{2}{\alpha_0} t^{\frac{2}{\alpha_0}} B\left(1 - \frac{2}{\alpha_0}, \frac{2}{\alpha_0}, \frac{t}{1+t}\right)\right)} dt, \quad (9)$$

$$\begin{aligned} f_s(T_n) &= W_s \pi \lambda_1 T_n \int_0^{\infty} \int_0^{R_c^2} \frac{S^t(N_1, k)}{t} \\ &\times \exp\left(Z^{x,t} \left(\frac{1}{1+t}, \frac{t}{1+t}, \frac{x^{\frac{\alpha_1}{2}} t}{R_c^{\alpha_1} + x^{\frac{\alpha_1}{2}} t}\right)\right) dx dt, \end{aligned} \quad (10)$$

where

$$S^t(N_1, k) = \left(1 - \sum_{k=0}^{\infty} (1+t)^{-\max(N_1-k, 1)} p_K(k)\right), \quad (11)$$

$$\begin{aligned} Z^{x,t}(u, y, z) &= -\pi \lambda_1 x T_n \\ &+ x (\varepsilon (1 - T_n) C_2^t(u) + \varepsilon C_1^t(y) + (1 - \varepsilon) C_1^t(z)), \end{aligned} \quad (12)$$

$C_z^t(u) = -\pi \lambda_z t^{\frac{2}{\alpha_z}} \frac{2}{\alpha_z} B\left(1 - \frac{2}{\alpha_z}, \frac{2}{\alpha_z}, u\right)$, $z \in \{0, 1\}$, $C_2^t(u) = -\pi \lambda_1 t^{\frac{2}{\alpha_1}} \frac{2}{\alpha_1} B\left(\frac{2}{\alpha_1}, 1 - \frac{2}{\alpha_1}, u\right)$, and $B(x, y, z) = \int_0^z u^{x-1} (1-u)^{y-1} du$ is the incomplete Beta function.

proof 1: When the typical user u_0 requests file n , based on the capacity calculation lemma in [18], spectral efficiency is given by

$$\begin{aligned} R_z^n &= \mathbb{E}[\ln(1 + \text{SIR}_z)] \\ &= \int_0^{\infty} \int_0^{\infty} \frac{\mathcal{L}_{I_z}(t | |x_{z,0}|)}{t} (1 - \mathcal{L}_{S_z}(t | |x_{z,0}|)) f_{x_{z,0}}(x) dt dx, \end{aligned} \quad (13)$$

where $z \in \{0, 1\}$, and $\mathcal{L}_X(t)$ is the Laplace transform of X . Based on (13), we calculate R_0^n and R_1^n , respectively.

To begin with, based on the void probability of PPP, the probability density function (PDF) of the service distances in two layers can be calculated as follows:

$$f_{x_{0,0}}(x) = 2\pi\lambda_0 x \exp(-\pi\lambda_0 x^2),$$

$$f_{x_{1,0}}(x | x_{1,0} < R_c) = \frac{2\pi\lambda_1 T_n x \exp(-\pi T_n \lambda_1 x^2)}{1 - \exp(-\pi T_n \lambda_1 R_c^2)}, \quad (14)$$

and the cache hit probability P_s^n can be derived as follows:

$$P_s^n = 1 - P_m^n = \int_0^{R_c} 2\pi T_n \lambda_1 r e^{-\pi T_n \lambda_1 r^2} dr = 1 - e^{-\pi T_n \lambda_1 R_c^2}. \quad (15)$$

To obtain R_0^n , we first calculate the Laplace transforms of S_0 and I_0 , respectively. We rewrite the expressions of S_0 and I_0 in (3) as $S_0 = g_{x_{0,0}}$ and $I_0 = \sum_{x_{0,j} \in \Phi_0 \setminus x_{0,0}} g_{x_{0,j}} |x_{0,j}|^{-\alpha_0} |x_{0,0}|^{\alpha_0}$, respectively.

As $g_{x_{0,0}}$ is Gamma distributed, we obtain $\mathcal{L}_{S_0}(t | x_{0,0})$ as follows:

$$\mathcal{L}_{S_0}(t | x_{0,0}) = \mathbb{E}_{g_{x_{0,0}}} [e^{-g_{x_{0,0}} t}] = (1+t)^{-N_0}. \quad (16)$$

By applying the probability generating function (PGFL) of PPP, we derive the Laplace transform of I_0 as follows:

$$\mathcal{L}_{I_0}(t | x_{0,0}) = \exp\left(C_0^t \left(\frac{t}{1+t}\right) |x_{0,0}|^2\right). \quad (17)$$

Then, by substituting (14), (16) and (17) into (13), we can obtain R_0^n after some algebraic manipulations.

To obtain R_1^n , we first calculate the Laplace transforms of S_1 and I_1 , respectively. We rewrite the expressions of S_1 and I_1 in (4) as $S_1 = g_{x_{1,0}}$ and $I_1 = \sum_{x_{1,j} \in \Phi_1^1 \cup \Phi_1^2 \cup \Phi_1^3} g_{x_{1,j}} |x_{1,j}|^{-\alpha_1} |x_{1,0}|^{\alpha_1}$, respectively. Based on the law of total expectation, the Laplace transform of S_1 is given by

$$\mathcal{L}_{S_1}(t | x_{1,0}) = \sum_{k=0}^{\infty} (1+t)^{-\max(N_1-k, 1)} p_K(k). \quad (18)$$

In order to calculate the Laplace transform of I_1 , we define $I_1 = I_1^1 + I_1^2 + I_1^3$, where $I_1^z = \sum_{x_{1,j} \in \Phi_1^z} |x_{1,0}|^{\alpha_1} |x_{1,j}|^{-\alpha_1} g_{x_{1,j}}$, and $z \in \{1, 2, 3\}$. First, using the PGFL of PPP with densities (7) in different regions, we calculate the Laplace transforms of three types of interferences as follows:

$$\begin{aligned} & \mathcal{L}_{I_1^1}(t | x_{1,0}) \\ &= \exp\left(-2\pi\epsilon(1-T_n)\lambda_1 \int_0^{|x_{1,0}|} \left(1 - \frac{1}{1+|x_{1,0}|^{\alpha_1} r^{-\alpha_1} t}\right) r dr\right) \\ &= \exp\left(\epsilon(1-T_n)C_2^t \left(\frac{1}{1+t}\right) |x_{1,0}|^2\right), \\ & \mathcal{L}_{I_1^2}(t | x_{1,0}) = \exp\left(-2\pi\epsilon\lambda_1 \int_0^{R_c} \left(1 - \frac{1}{1+|x_{1,0}|^{\alpha_1} r^{-\alpha_1} t}\right) r dr\right) \\ &= \exp\left(\epsilon\left(C_1^t \left(\frac{t}{1+t}\right) - C_1^t \left(\frac{|x_{1,0}|^{\alpha_1} R_c^{-\alpha_1} t}{1+|x_{1,0}|^{\alpha_1} R_c^{-\alpha_1} t}\right)\right) |x_{1,0}|^2\right), \\ & \mathcal{L}_{I_1^3}(t | x_{1,0}) = \exp\left(-2\pi\lambda_1 \int_{R_c}^{\infty} \left(1 - \frac{1}{1+|x_{1,0}|^{\alpha_1} r^{-\alpha_1} t}\right) r dr\right) \\ &= \exp\left(C_1^t \left(\frac{|x_{1,0}|^{\alpha_1} R_c^{-\alpha_1} t}{1+|x_{1,0}|^{\alpha_1} R_c^{-\alpha_1} t}\right) |x_{1,0}|^2\right). \end{aligned} \quad (19)$$

Then, we can calculate the Laplace transform of I_1 as $\mathcal{L}_{I_1}(t | x_{1,0}) = \mathcal{L}_{I_1^1}(t | x_{1,0}) \mathcal{L}_{I_1^2}(t | x_{1,0}) \mathcal{L}_{I_1^3}(t | x_{1,0})$. We omit the details here due to the space limitation. By substituting $\mathcal{L}_{I_1}(t | x_{1,0})$, (14), and (18) into (13), we can obtain R_1^n after some algebraic manipulations.

Finally, by substituting R_0^n , R_1^n and (15) into (5), we can obtain the per-user throughput.

Note that if each SBS adopts MRT precoding instead of ZFBF, the per-user throughput can be obtained easily by Theorem 1. Moreover, our analytical result (8) does not contain the high order derivatives of the Laplace transform as in [13] and the matrix inversion as in [12], [15], thus it can be easily calculated by mathematical software. Under the parameters in Section V, the computation time using Monte-Carlo simulations is more than 500 times of that using our analytical results, which demonstrates that our results are more efficient and tractable than Monte-Carlo simulations.

IV. THROUGHPUT MAXIMIZATION

In this section, we design the caching placement \mathbf{T} in our scheme by solving the following optimization problem:

$$\mathbf{P0} : \max_{\mathbf{T}} R(\mathbf{T}) = \sum_{n \in \mathcal{F}} a_n (f_m(T_n) + f_s(T_n)) \quad (20a)$$

$$\text{s.t.} \quad \sum_{n \in \mathcal{F}} T_n \leq C, \quad (20b)$$

$$0 \leq T_n \leq 1, n \in \mathcal{F}. \quad (20c)$$

Since storing more files will increase the per-user throughput, without loss of optimality, we rewrite the constraint (20b) as follows:

$$\sum_{n \in \mathcal{F}} T_n = C. \quad (21)$$

Notice that it is difficult to ensure the convexity of $R(\mathbf{T})$ in general, due to the summation of two tiers and the complex structure of $f_s(T_n)$. However, problem $\mathbf{P0}$ is a continuous optimization of a differentiable function over a convex set, since function $R(\mathbf{T})$ is differentiable and the constraints in (20c) (21) are linear. Therefore, we can use the gradient projection method in [9] to compute a local-optimal solution (local-Opt.).

To obtain some design insights, we first consider a special case with $W_s \gg W_m$, since more users will be associated with an MBS than an SBS in the traditional HetNets, which makes the available bandwidth of an SBS for u_0 is larger than that of an MBS in general [10]. In this case, since the impact of the throughput contributed by MBS tier can be safely ignored, we consider the throughput maximization problem as follows:

$$\mathbf{P1} : \max_{\mathbf{T}} \underline{R}(\mathbf{T}) = \sum_{n \in \mathcal{F}} a_n f_s(T_n)$$

$$\text{s.t.} \quad \sum_{n \in \mathcal{F}} T_n = C, \quad 0 \leq T_n \leq 1, n \in \mathcal{F}. \quad (22)$$

However, it is still difficult to ensure the convexity of $\underline{R}(\mathbf{T})$ in general case due to the complex form of $f_s(T_n)$. To further simplify $\mathbf{P1}$, we consider a special case that $R_c \leq \sqrt{\frac{2}{\pi\lambda_1}}$ and $N_1 > 4$. Note that this means that the average number of IN requests received by a SBS is less than 2, which is close to

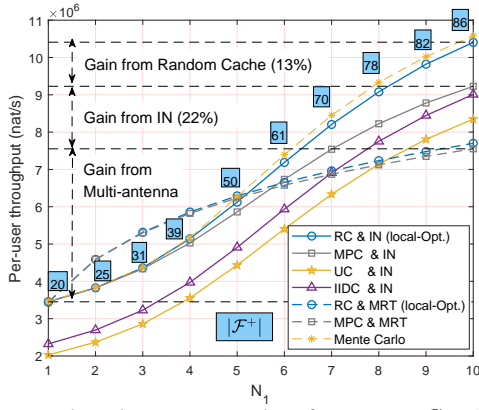


Fig. 1. Per-user throughput versus number of antennas at $C = 20$, $\gamma = 0.5$, and $R_c = 100$.

the best value as shown in [15]. Meanwhile, in a realistic scenario, the size of the coordinated set would not be large due to the signaling overhead. In this case, due to $\varepsilon \rightarrow 0$, the second order derivative of the objective function $\underline{R}(\mathbf{T})$ with respect to T_n can be expressed as:

$$\frac{\partial^2 \underline{R}(\mathbf{T})}{T_n^2} = a_n W_s \pi^2 \lambda_1^2 \int_0^\infty \int_0^{R_c} \frac{S^t(N_1, k)}{t} (T_n \pi \lambda_1 x - 2) \times \exp\left(Z^{x,t} \left(\frac{1}{1+t}, \frac{t}{1+t}, \frac{x^{\alpha_1} t^{\frac{\alpha_1}{2}}}{R_c^{\alpha_1 + x^{\frac{\alpha_1}{2}} t}}\right)\right) x dx dt. \quad (23)$$

It is easy to verify that $\frac{\partial^2 \underline{R}(\mathbf{T})}{T_n^2} \leq 0$ when $R_c \leq \sqrt{\frac{2}{\pi \lambda_1}}$, thus $\mathbf{P1}$ is convex. Therefore, we can obtain the near-optimal solutions (near-Opt.) to $\mathbf{P0}$ by solving $\mathbf{P1}$, since the optimal objective value obtained from $\mathbf{P1}$ in general serves as a tight lower bound of that of problem $\mathbf{P0}$. Using Karush-Kuhn-Tucker (KKT) condition, the near-optimal solutions to $\mathbf{P0}$ are given by

$$T_n^*(\nu^*) = [\xi(\nu^*)]_0^1, \quad n \in \mathcal{F}, \quad (24)$$

where $[x]_0^1 \triangleq \max\{\min\{x, 1\}, 0\}$, and $\xi(\nu^*)$ is the solution over T_n of the equation $a_n f_s'(T_n^*) = \nu^*$. The optimal Lagrange multiplier ν^* can be obtained by bisection search based on the condition $\sum_{n \in \mathcal{F}} T_n^*(\nu^*) = C$.

Based on (24), since $f_s'(T_n)$ is a decreasing function and we have $a_1 \geq a_2 \geq \dots \geq a_F \geq 0$, we can easily obtain that $1 \geq T_1^* \geq T_2^* \geq \dots \geq T_F^* \geq 0$. This indicates that SBSs tend to cache popular files, which is consistent with our intuition.

V. NUMERICAL RESULTS

In this section, numerical results are presented to compare our proposed scheme, i.e., RC combined with IN (RC&IN), with some existing baseline schemes. Unless otherwise noted, our simulation is based on the following setting: $W_m = 0.2$ MHz, $W_s = 5$ MHz, $N_0 = 10$, $N_1 = 7$, $\lambda_u = \frac{1}{52\pi} \text{m}^{-2} = 10^2 \lambda_1 = 10^4 \lambda_0$, $\alpha_0 = \alpha_1 = 4$, $F = 100$, $C = 20$, $R_c = 100\text{m}$, and the Zipf exponent $\gamma = 0.5$. We obtain the Monte-Carlo results by averaging over 10^4 random realization.

Fig. 1 shows the impact of physical-layer related parameter N_1 on caching performance, it also verifies our throughput expression with Monte-Carlo simulations. Fig. 1 demonstrates

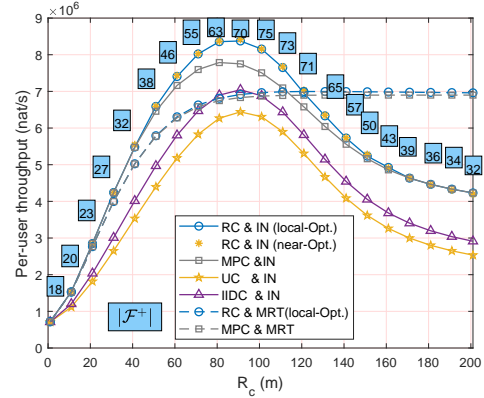


Fig. 2. Per-user throughput versus cooperation radius at $C = 20$, $\gamma = 0.5$ and $N_1 = 7$.

that without IN, the file diversity gain (FDG) (the gap between RC&MRT and MPC&MRT) is negligible due to the overwhelming interference. In contrast, FDG (the gap between RC&IN and MPC&IN) is obvious with IN. Fig. 1 also shows that both the FDG (the gap between RC&IN and MPC&IN) and cooperation gain (the gap between RC&IN and RC&MRT) benefit from IN, especially at large N_1 . This is because increasing N_1 enhances the ability of IN, reduces interference residual ratio ε , and protects the performance when users download less popular files from farther SBSs. Particularly, we can observe that when N_1 is relatively small or R_c is relatively large, it is better to switch to the non-coordination case, i.e., adopting MRT precoding to enhance its desired signal, because of the small effective channel gain and the large ε in these regions. Moreover, it is observed that more different contents can be cached in the SBS tier when SBSs are equipped with more antennas.

Fig. 2 shows the impact of physical-layer related parameter R_c on caching performance. It also demonstrates that our near-optimal solutions are very close to our local-optimal solutions, even at large R_c region. It also shows that the optimal R_c is around $\sqrt{2/(\pi \lambda_1)}$. In addition, it is observed that our proposed design first increases and then decreases when R_c increases. The reason lies in that increasing R_c can first grow the cache hit probability while eliminating more interference. However, when R_c becomes large enough, the SBS only has a small DoF for its own signal links, and the interference residual ratio is high. Moreover, we can observe that RC will reduce to MPC when R_c is small or sufficiently large. This is because when R_c is small, the MPC scheme can bring the largest cache hit probability. When R_c is sufficiently large, the cache hit probability and ε is very large, thus users tend to be associated with the nearest SBS to avoid the heavy interference. Furthermore, it is observed that more different files cached (i.e., larger $|\mathcal{F}^+|$) leads to larger FDG (the gap between RC&IN and MPC&IN).

Fig. 3 and Fig. 4 show the impact of content-layer related parameters on caching performance. It is observed that RC&IN can fully harvest the FDG compared to RC without IN, since it effectively mitigates the dominant interferences.

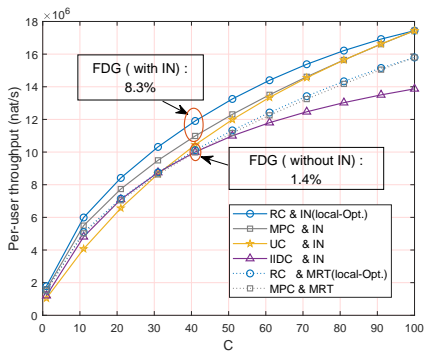


Fig. 3. Per-user throughput versus cache size at $R_c = 100$ and $\gamma = 0.5$.

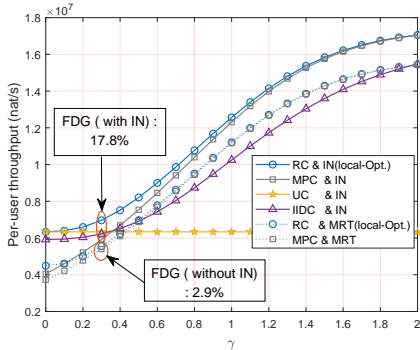


Fig. 4. Per-user throughput versus Zipf exponent at $R_c = 100$ and $C = 20$.

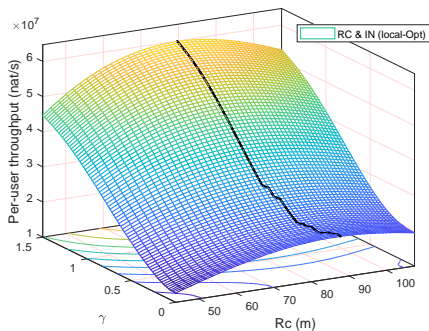


Fig. 5. Per-user throughput under RC&IN scheme.

It is also observed that our proposed design is superior to all the contrastive schemes. Particularly, Fig. 3 shows that cooperation gain (the gap between RC&IN and RC&MRT) and throughput of all the schemes increase with cache size. This is because large cache size increases the cache hit probability, more files can be downloaded from the nearest SBSs, thus increasing the throughput. Meanwhile, to gain FDG, large cache size also increases the cache probabilities of those less popular files, thereby increasing the benefits from IN. Fig. 4 shows that optimal cache placement changes from UC to MPC with increasing γ . This is because large γ means that the content requirements become more concentrated, thus SBSs only need to cache the most popular files.

Fig. 5 shows the relationship between content-layer related parameter γ and physical-layer related parameter R_c . The black line represents the maximum value of throughput versus γ . It is observed that optimal R_c decreases when γ increases, which means that UC scheme need larger cooperation region

than MPC scheme. The reason lies in that under a more concentrated file request, users may find their desired files in a closer SBS, thus decreasing the optimal cooperation radius.

VI. CONCLUSION

In this paper, we jointly considered random cache and interference nulling in multi-antenna HetNets. The explicit expression of the throughput was first obtained by using tools from stochastic geometry. Then, we tackled the throughput maximization problem under cache distribution. Numerical results showed that joint random cache and IN can sufficiently reap the file diversity gain and achieve a significant gain in the per-user throughput over existing baseline schemes.

REFERENCES

- [1] J. G. Andrews *et al.*, "What will 5G be?" *IEEE J. Sel. Areas Commun.*, vol. 32, no. 6, pp. 1065–1082, Jun. 2014.
- [2] L. Li, G. Zhao, and R. S. Blum, "A survey of caching techniques in cellular networks: Research issues and challenges in content placement and delivery strategies," *IEEE Commun. Surveys Tuts.*, vol. 20, no. 3, pp. 1710–1732, 3rd Quarter 2018.
- [3] E. Baştuğ, M. Bennis, M. Kountouris, and M. Debbah, "Cache-enabled small cell networks: Modeling and tradeoffs," *EURASIP J. Wireless Commun. Netw.*, vol. 2015, no. 1, p. 41, 2015.
- [4] H. Wu, N. Zhang, Z. Wei *et al.*, "Content-aware cooperative transmission in HetNets with consideration of base station height," *IEEE Trans. Veh. Technol.*, vol. 67, no. 7, pp. 6048–6062, Jul. 2018.
- [5] T. ul Hassan *et al.*, "Caching in wireless small cell networks: A storage-bandwidth tradeoff," *IEEE Commun. Lett.*, vol. 20, no. 6, pp. 1175–1178, Jun. 2016.
- [6] B. B. Nagaraja and K. G. Nagananda, "Caching with unknown popularity profiles in small cell networks," in *Proc. IEEE Glob. Commun. Conf. (GlobeCom)*, San Diego, CA, USA, Dec. 2015, pp. 1–6.
- [7] Z. Chen, N. Pappas, and M. Kountouris, "Probabilistic caching in wireless D2D networks: Cache hit optimal versus throughput optimal," *IEEE Commun. Lett.*, vol. 21, no. 3, pp. 584–587, Mar. 2017.
- [8] J. Wen, K. Huang, S. Yang, and V. O. Li, "Cache-enabled heterogeneous cellular networks: Optimal tier-level content placement," *IEEE Trans. Wireless Commun.*, vol. 16, no. 9, pp. 5939–5952, Sep. 2017.
- [9] Y. Cui, D. Jiang, and Y. Wu, "Analysis and optimization of caching and multicasting in large-scale cache-enabled wireless networks," *IEEE Trans. Wireless Commun.*, vol. 15, no. 7, pp. 5101–5112, Jul. 2016.
- [10] W. Wen, Y. Cui, F.-C. Zheng, S. Jin, and Y. Jiang, "Random caching based cooperative transmission in heterogeneous wireless networks," *IEEE Trans. Commun.*, vol. 66, no. 7, pp. 2809–2825, Jul. 2018.
- [11] S. H. Chae, T. Q. Quek, and W. Choi, "Content placement for wireless cooperative caching helpers: A tradeoff between cooperative gain and content diversity gain," *IEEE Trans. Wireless Commun.*, vol. 16, no. 10, pp. 6795–6807, Oct. 2017.
- [12] S. Kuang and N. Liu, "Random caching in backhaul-limited multi-antenna networks: Analysis and area spectrum efficiency optimization," *arXiv preprint arXiv:1709.06278*, 2017.
- [13] X. Xu and M. Tao, "Analysis and optimization of probabilistic caching in multi-antenna small-cell networks," in *Proc. IEEE Glob. Commun. Conf. (GlobeCom)*, Singapore, Dec. 2017, pp. 1–6.
- [14] J. Park, N. Lee, and R. W. Heath, "Cooperative base station coloring for pair-wise multi-cell coordination," *IEEE Trans. Commun.*, vol. 64, no. 1, pp. 402–415, Jan. 2016.
- [15] C. Li, J. Zhang, M. Haenggi, and K. B. Letaief, "User-centric intercell interference nulling for downlink small cell networks," *IEEE Trans. Commun.*, vol. 63, no. 4, pp. 1419–1431, Apr. 2015.
- [16] Y. Cui, Y. Wu, D. Jiang, and B. Clerckx, "User-centric interference nulling in downlink multi-antenna heterogeneous networks," *IEEE Trans. Wireless Commun.*, vol. 15, no. 11, pp. 7484–7500, Nov. 2016.
- [17] G. Chen, L. Qiu, and Y. Li, "Stochastic geometry analysis of coordinated beamforming small cell networks with CSI delay," *IEEE Commun. Lett.*, vol. 22, no. 5, pp. 1066–1069, May 2018.
- [18] K. A. Hamdi, "A useful lemma for capacity analysis of fading interference channels," *IEEE Trans. Commun.*, vol. 58, no. 2, pp. 411–416, Feb. 2010.